


 Cite this: *RSC Adv.*, 2026, 16, 7967

 Received 9th January 2026
 Accepted 30th January 2026

DOI: 10.1039/d6ra00218h

rsc.li/rsc-advances

Molecular iodine catalyzed C3-quaternization *via* oxidative dearomatization of indoles: direct access to 3,3-di(indolyl)indolin-2-ones

 Neetika Singh,  Hari Prasad Kokatla, * Nagaraju Naddi  and Madhu Inapanuri 

An efficient and sustainable method for the synthesis of 3,3-di(indolyl)indolin-2-one derivatives has been developed *via* iodine-catalyzed oxidative dearomatization, where indole alone directly participates in the reaction. Utilising iodine as a green oxidant and DMSO as the optimal solvent, the reaction proceeds under mild conditions, eliminating the need for pre-functionalized indoles and minimising waste, aligning with green chemistry principles. The optimized protocol demonstrates broad substrate scope, high yields, and excellent selectivity, tolerating various functional groups.

Introduction

The oxindole framework is a privileged heterocyclic scaffold frequently encountered in natural products, pharmaceuticals, and bioactive molecules, and has received considerable attention in synthetic and medicinal chemistry.^{1,2} Within this class, 3,3-disubstituted oxindoles are particularly important owing to their structural rigidity, extended π -conjugation, and nitrogen-rich environment.^{3,4} These attributes align them with pharmacologically relevant scaffolds and underpin their diverse biological activities, including spermicidal,⁵ antimicrobial,⁶ enzyme inhibition,^{7–9} and anticancer properties (Fig. 1).^{10–12}

Among the known derivatives, 3,3-di(indolyl)indolin-2-ones represent a compelling subclass, wherein two indole moieties are anchored at the C3-position of an oxindole synthon. Indolin-2-one and indolin-3-one scaffolds have attracted considerable attention due to their presence in numerous bioactive natural

products and pharmaceuticals.^{13,14} Within this framework, the synthesis of C2-quaternary indolin-3-ones has been widely studied, leading to diverse and efficient methodologies.^{15–19} In contrast, the chemistry of C3-quaternary indolin-2-ones has remained relatively limited, despite their potential significance. This gap underscores the opportunity for further methodological development to access these valuable structural motifs, which impart distinct steric and electronic features, making them highly valuable for medicinal chemistry applications.

Existing strategies toward 3,3-di(indolyl)indolin-2-ones require prefunctionalized indoles such as isatins,²⁰ oxindole²¹ or 3-diazo oxindoles,²² as well as pseudomulticomponent²³ strategies that demand specialised reagents. The most widely adopted strategies are the condensation of isatins with indoles in the presence of catalysts such as acidic promoters (*e.g.*, silica sulfuric acid,²⁴ Amberlyst-15,²⁵ TsOH,²⁶ cellulose sulfuric acid,²⁷ HFIP²⁸), metal-based catalysts (*e.g.*, FeCl₃,²⁹ CAN,³⁰ nanocrystalline MgAl₂O₄,³¹ silica-supported In(acac)₃,³² and palladium nanoparticles.³³ However, Liu *et al.* developed a method for the synthesis of 3,3-biindoline-2-ones by silver/TEMPO catalytic system, and they observed trace amounts of the 3,3-di(indolyl)indolin-2-ones.³⁴ Although these approaches can deliver the desired framework, they often suffer from poor atom economy, restricted substrate scope, and operational complexity.

In recent years, oxidative strategies have attracted increasing attention as viable alternatives for accessing oxindole architectures. In this context, iodine-based systems, particularly the I₂/DMSO combination, have emerged as powerful platforms for indole functionalization through oxidative dearomatization pathways. The I₂/DMSO system has been successfully employed for the oxygenation of indoles to afford isatins as well as for iodine-catalyzed oxidative coupling of indolin-2-ones with indoles to generate 3,3-disubstituted oxindole frameworks.^{35–37} While these reports highlight the efficiency of I₂/DMSO systems, they predominantly rely on pre-oxidized intermediates or

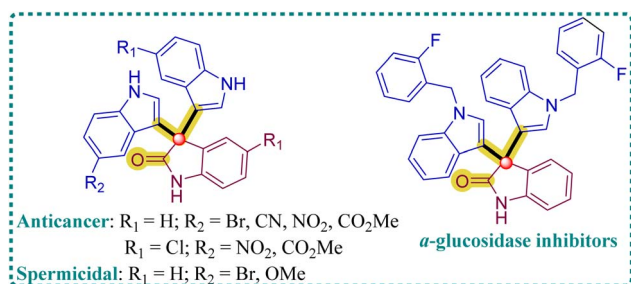
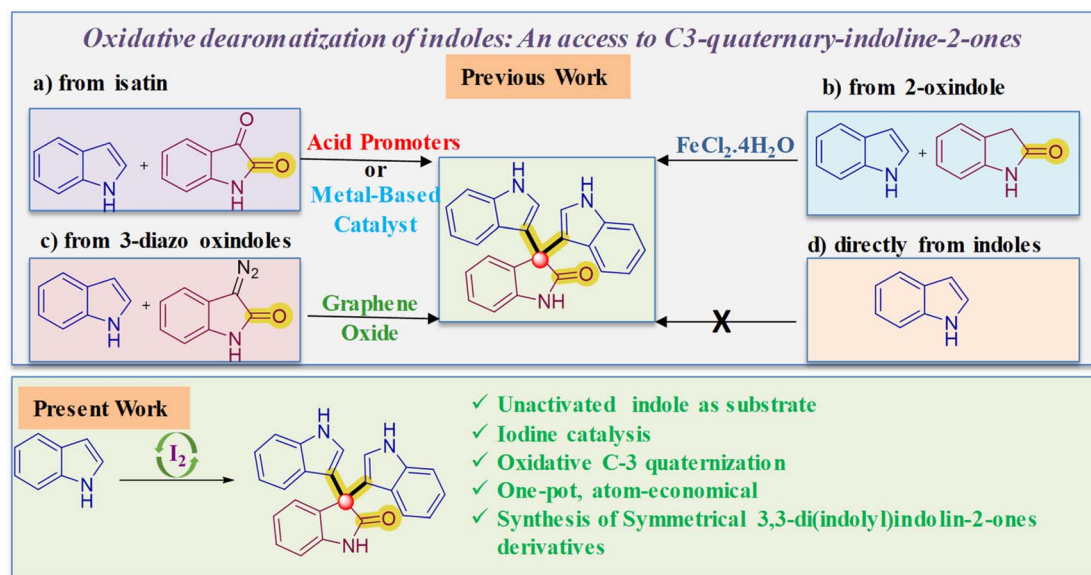


Fig. 1 Representative examples of pharmacologically active 3,3-bi(indol-3-yl)indolinones.

Department of Chemistry, National Institute of Technology Warangal, Warangal, Telangana-506004, India. E-mail: harikokatla@nitw.ac.in





Scheme 1 Strategies for the formation of C3-quaternary indolin-2-ones.

specific substrate classes, leaving substantial scope for the development of complementary strategies that enable direct C3-quaternization from simple indoles under milder and more sustainable conditions.

In this context, molecular iodine stands out as an attractive reagent, being mild, inexpensive, and environmentally benign, with wide utility in oxidative transformations.³⁸ Our group has previously demonstrated the usefulness of iodine catalysis in

Table 1 Optimization studies^a

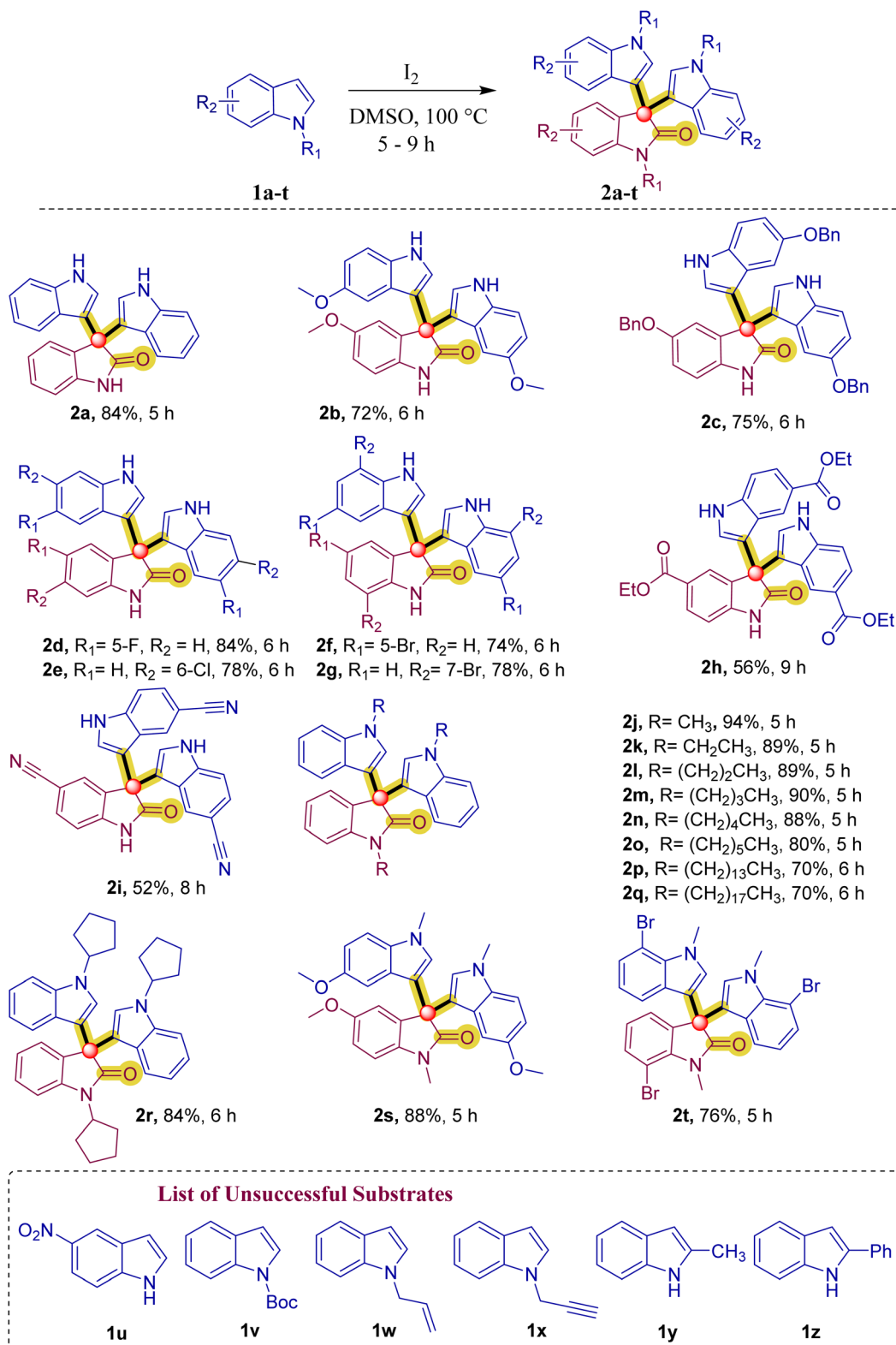
Entry	Catalyst	Solvent	Temp. (°C)	Time (h)	Yield (%) ^b
1	I ₂	CH ₂ Cl ₂	30	12	n.r. ^c
2	I ₂	CHCl ₃	50	12	n.r. ^c
3	I ₂	THF	100	10	n.r. ^c
4	I ₂	CH ₃ CN	70	8	n.r. ^c
5	I ₂	Toluene	100	12	n.r. ^c
6	I ₂	EtOH	60	24	n.r. ^c
7	I ₂	DMF	100	12	n.r. ^c
8	I ₂	H ₂ O	90	24	n.r. ^c
9	I ₂	DMSO	100	5	84
10	I ₂	DMSO	100	7	59 ^d
11	I ₂	DMSO	100	7	77 ^e
12	I ₂	DMSO	100	7	53 ^f
13	I ₂	DMSO	100	7	53 ^g
14	I ₂	DMSO	100	8	33 ^h
15	I ₂	DMSO	100	8	32 ⁱ
16	NIS	DMSO	100	8	40
17	KI	DMSO	100	24	n.r. ^c

^a Reaction conditions: indole (1.0 mmol), catalyst (10 mol%), solvent (2 mL), stirred at the specified temperature under open atmosphere. ^b Isolated yields. ^c n.r. = no reaction. ^d 2 mol%. ^e 5 mol%. ^f 15 mol%. ^g 20 mol%. ^h 25 mol%. ⁱ 30 mol%.



C–H functionalization, exemplified by the iodine-catalysed C2–H formamidation of quinoline *N*-oxides using isocyanides.³⁹ Motivated by these results, we envisaged extending iodine-

mediated oxidative strategies to achieve direct dearomatization for the construction of C3-quaternary indolin-2-ones (Scheme 1).



Scheme 2 Substrate scope^{a,b}. ^aReaction conditions: All the reactions were conducted on a 1.0 mmol scale of **1a–t** (1.0 mmol) and iodine (10 mol%) in DMSO solvent (2 mL) at 100 °C. ^bIsolated yields.



Herein, we describe an operationally simple, iodine-mediated oxidative dearomatization methodology that provides direct, metal-free, and atom-economical access to 3,3-di(indolyl)indolin-2-ones directly from indoles. This strategy eliminates the need for preactivated substrates, proceeds under mild conditions, and delivers products with high selectivity, establishing a sustainable platform for the synthesis of biologically relevant scaffolds.

Results and discussion

In our preliminary investigations, we sought to establish an efficient protocol for the synthesis of 3,3-di(indolyl)indolin-2-one **2a** using indole **1a** (1.0 mmol) and iodine as a catalyst. The reaction was initially examined in a variety of common organic solvents employing I₂ (10 mol%) under thermal conditions. However, non-polar and moderately polar solvents such as CH₂Cl₂, CHCl₃, THF, CH₃CN, toluene, EtOH, DMF, and H₂O failed to promote the desired transformation, and no reaction was observed even after prolonged heating (Table 1, entries 1–8). Gratifyingly, a dramatic solvent effect was observed when the reaction was conducted in DMSO. Under these conditions, the desired product **2a** was obtained in an excellent 84% yield within 5 h at 100 °C (Table 1, entry 9). The superior performance of DMSO can be attributed to its high polarity and ability to stabilize iodine-derived reactive intermediates, thereby facilitating efficient C–C bond formation. The structure of **2a** was unambiguously confirmed by ¹H NMR, ¹³C NMR, DEPT-135, and HRMS analyses (see SI).

Subsequently, the influence of iodine loading was examined in DMSO. Reducing the catalyst loading to 2 and 5 mol% resulted in diminished yields of 59% and 77%, respectively, after 7 h, indicating incomplete conversion under these conditions (Table 1, entries 10 and 11). Conversely, increasing the iodine loading beyond the optimal 10 mol% proved detrimental. Higher catalyst loadings (15–30 mol%) led to a significant decrease in product yield (32–53%; Table 1, entries 12–15), presumably due to competitive side reactions or overoxidation processes induced by excess iodine.

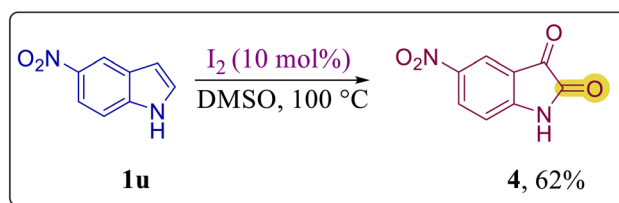
Other iodine sources were also evaluated. *N*-iodosuccinimide (NIS) afforded only a moderate 40% yield under otherwise identical conditions (Table 1, entry 16), while potassium iodide (KI) was completely ineffective, showing no reaction even after 24 h (Table 1, entry 17).

Overall, these optimization studies highlight the crucial interplay of solvent polarity, iodine stoichiometry, and temperature in maximizing the efficiency of this iodine-mediated indole coupling reaction. Once the optimal conditions were established, we extended our study to explore the scope of the reaction with a variety of indole derivatives (Scheme 2). Under the optimized reaction conditions, 1*H*-indole **1a** underwent a smooth transformation to afford the corresponding product **2a** in excellent yield (Scheme 2), demonstrating the baseline reactivity of the parent scaffold. Electron-donating groups on the benzene ring, such as 5-methoxy-1*H*-indole **1b** and 5-(benzyloxy)-1*H*-indole **1c** substituents, were well tolerated, affording the desired products **2b–2c** in good yields

(Scheme 2). These results highlight the method's compatibility with electron-rich aromatic systems.

Similarly, halogens such as fluoro, chloro, and bromo at various positions on the benzene ring **1d–1g** also underwent efficient transformation to deliver the corresponding products **2d–2g** in moderate-to-good yields 74–84% (Scheme 2). The successful incorporation of halogenated indoles underscores the robustness of the protocol and its potential for further synthetic elaboration.

However, indoles bearing electron-withdrawing substituents, such as ethyl 1*H*-indole-5-carboxylate **1h** and 1*H*-indole-5-carbonitrile **1i**, exhibited reduced reactivity, affording the corresponding products **2h** and **2i** (Scheme 2) in only 56% and 52% yields, respectively, likely due to decreased electron density on the aromatic ring, adversely affecting the reaction efficiency. Notably, nitro-substituted indoles **1u** predominantly yielded the corresponding NO₂-isatin **4** (Scheme 3) instead of the 5,5',5''-trinitro-[3,3':3'',3'''-terindolin]-2'-one and the NMR data confirming the formation of the NO₂-substituted isatin **4** are provided in the SI. This behaviour indicates that although substrate consumption occurs, the intrinsic reactivity of electron-deficient indoles favours overoxidation rather than controlled C3-quaternization. Furthermore, a broad range of *N*-alkylated indoles bearing various alkyl chains, including methyl, ethyl, propyl, butyl, pentyl, hexyl, tetradecane, octadecane, and cyclopentyl **1j–1r** underwent smooth conversion, affording their respective products **2j–2r** (Scheme 2) in good-to-



Scheme 3 Conversion of 5-nitroindole to 5-nitroindoline-2,3-dione.

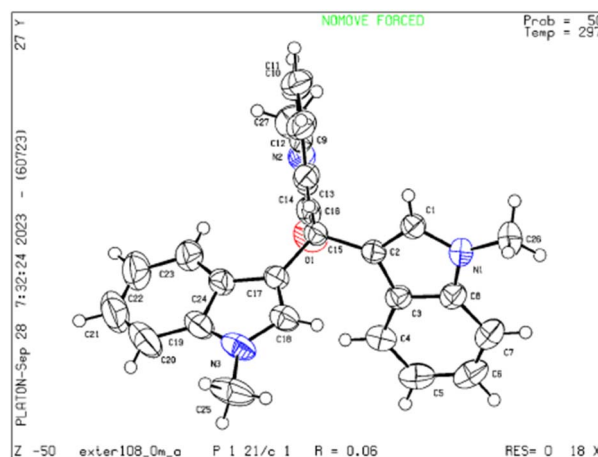
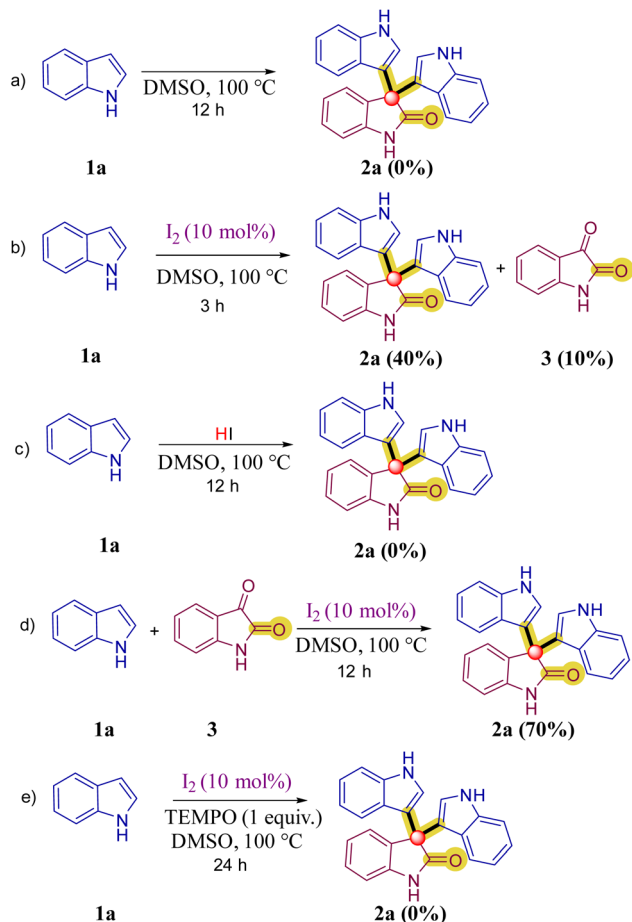


Fig. 2 ORTEP representations of X-ray crystal structures of 1,1',1''-trimethyl-1*H*,1'*H*-[3,3':3'',3'''-terindolin]-2'(1'*H*)-one **2j**. The thermal ellipsoids are drawn at a 50% probability level.





Scheme 4 Control experiments.

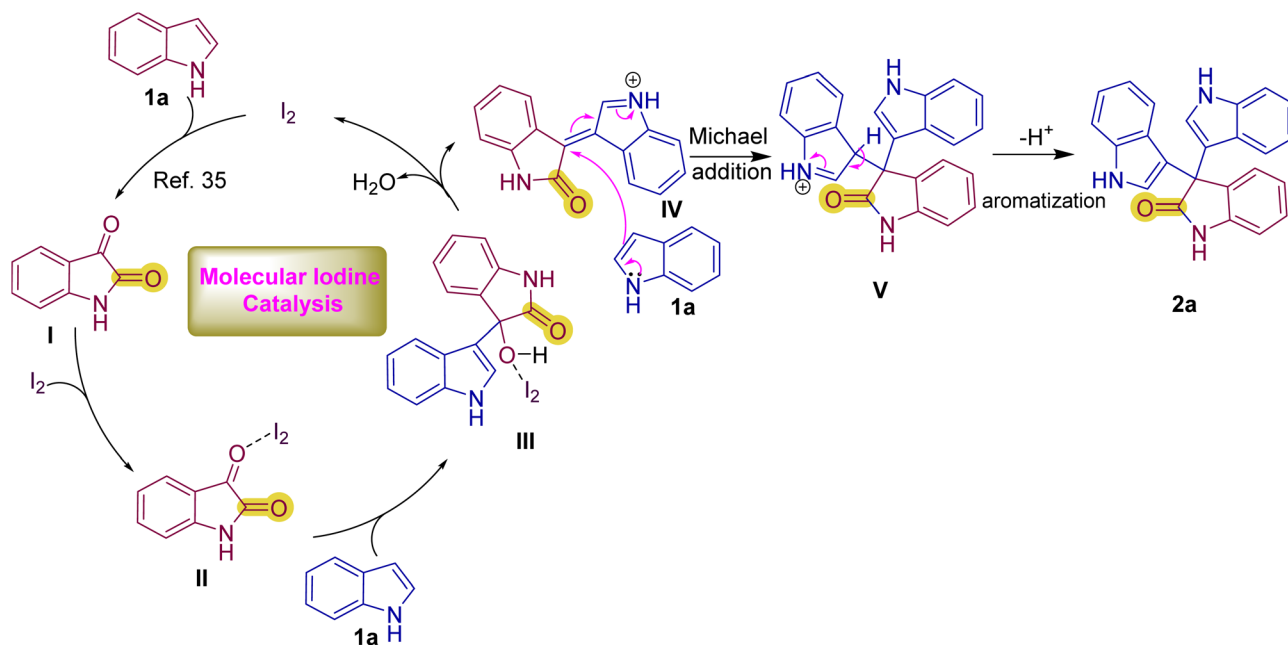
excellent yields. Notably, *N*-alkylated methoxy indole **1s** and *N*-alkylated bromo-substituted indole **1t** were also compatible under the reaction conditions, affording **2s** and **2t** (Scheme 2) in similarly high yields, highlighting the method's tolerance to both steric and electronic diversity at the nitrogen atom.

It is noteworthy that substrates bearing strong electron-withdrawing substituents, such as 5-nitroindole **1u** and *N*-Boc indole **1v**, failed to undergo the transformation, presumably because the electron-withdrawing groups significantly reduce the nucleophilicity of the indole core. Likewise, *N*-allyl indole **1w**, *N*-propargyl indole **1x** and C-2 substituted indoles **1y–1z** also proved unreactive, which may be attributed to potential interactions of the allyl or propargyl functionalities with iodine and blocking of substitutions on C-2 position (Scheme 2).

All synthesized compounds **2a–2t** (Scheme 2) were characterized using ¹H NMR, ¹³C NMR, and mass spectrometry. The molecular structure of compound **2j** was unambiguously confirmed through single-crystal X-ray diffraction (XRD) analysis (Fig. 2). Detailed crystallographic data and refinement parameters are provided in the SI (Table S1). This optimized protocol demonstrates excellent efficiency and broad substrate scope, allowing the synthesis of structurally diverse 3,3-di(indolyl)indolin-2-ones with high regioselectivity and yields.

The method is tolerant to various functional groups and provides a platform for further chemical modifications, showcasing its potential utility in synthetic and medicinal chemistry.

To elucidate the reaction mechanism, the control experiments were conducted to investigate the role of iodine and reactive intermediates, and the results are summarized in Scheme 4. Initially, the reaction of indole **1a** in DMSO at 100 °C, in the absence of iodine (10 mol%), was performed, which resulted in no formation of the desired product **2a**, highlighting the essential role of iodine in the transformation (Scheme 4a).



Scheme 5 Plausible reaction mechanism.



During the optimization of reaction conditions (Table 1), a yellow spot was observed on TLC and disappeared during the course of the reaction; this intermediate was isolated by quenching the reaction mixture at an early stage and was identified as isatin by comparison with an authentic sample. The formation of isatin **I** was further confirmed by NMR analysis, and the corresponding data are provided in the SI. These observations indicate that isatin is generated *in situ* through the reaction of indole **1a** with iodine (Scheme 4b). Additionally, the reaction of indole **1a** with HI alone did not afford the desired product, suggesting that HI is not competent to mediate the transformation (Scheme 4c).

To further validate the involvement of isatin as a key intermediate, preformed isatin was treated with indole **1a** under the standard reaction conditions, which resulted in the formation of the desired 3,3-di(indolyl)indoline-2-one **2a** in 70% yield, thereby confirming the feasibility of isatin in the proposed reaction pathway (Scheme 4d). Furthermore, when the reaction was carried out in the presence of the radical scavenger TEMPO, the formation of product **2a** was completely suppressed, and no product was detected (0% yield), indicating the possible involvement of a radical pathway in the reaction (Scheme 4e).

Based on the control experiments and literature reports,^{35,36} a plausible mechanism is outlined in Scheme 5. Initially, indole undergoes *in situ* oxidation by molecular iodine to form isatin **I**, which subsequently undergoes nucleophilic attack with indole at the C-3 position of isatin to generate intermediate **III**. Upon dehydration of intermediate **III**, a Michael acceptor 2-oxoindolin-3-ylidene-3*H*-indol-1-ium **IV** is formed. Subsequently, indole π electrons attack on intermediate **IV** *via* Michael addition to form intermediate **V**, which then undergoes aromatization to produce the desired product **2a** (Scheme 5).

Conclusions

In this study, we have developed an efficient, sustainable, and straightforward strategy for iodine-catalysed oxidative dearomatization to synthesise 3,3-di(indolyl)indolin-2-one derivatives directly from indoles. By using molecular iodine as a green oxidant in DMSO solvent, our method avoids the need for pre-functionalized substrates, reduces the number of reaction steps, and aligns with the principles of green chemistry. The protocol demonstrated a broad substrate scope, wide functional group tolerance, and the use of a green oxidising agent. This methodology not only expands the synthetic toolbox for accessing 3,3-di(indolyl)indolin-2-one scaffolds but also provides a foundation for further functionalization and exploration of these biologically significant compounds.

Author contributions

N. Singh and H. P. Kokatla designed the work, and N. Singh performed all the synthesis and characterization studies. N. Nagaraju and I. Madhu prepared the starting materials. All authors contributed to discussions. The manuscript was written by N. Singh and H. P. Kokatla.

Conflicts of interest

“There are no conflicts to declare”.

Data availability

CCDC 2490627 contains the supplementary crystallographic data for this paper.⁴⁰

The data supporting this article have been included as part of the supplementary information (SI). Experimental procedures, characterization data, and copies of the ¹H, ¹³C{¹H} and HRMS spectra of all compounds are included. Supplementary information is available. See DOI: <https://doi.org/10.1039/d6ra00218h>.

Acknowledgements

The author H.P.K. is grateful to the Anusandhan National Research Foundation (file nos. SERB-SCP/2022/000273, SERB-EEQ/2022/000511) and to the DST-FIST grant (SR/FST/CSII/2018/65) awarded to the Department of Chemistry, NIT Warangal, for financial support of this work. Neetika Singh gratefully acknowledges the Department of Science & Technology, Government of India, for financial support vide reference no. DST/WISE-PhD/CS/2024/38 (G) under the ‘DST-WISE Fellowship for PhD’ programme to carry out the research work. Central Research Instrumentation Facility (CRIF), for NMR and HRMS analysis, and NIT Warangal for infrastructure are acknowledged.

Notes and references

- 1 Y. M. Khetmalis, M. Shivani, S. Murugesan and K. V. G. Chandra Sekhar, *Biomed. Pharmacother.*, 2021, **141**, 111842.
- 2 M. Zhang, Y. Li, Y. Wang, J. Shu, T. Zhang, D. Zhang, S. Cai, T. Shi and W. Hu, *Green Synth. Catal.*, 2024, **5**, 180–185.
- 3 H. Suzuki, K. Sekino, S. Kondo, R. Minamikawa and T. Matsuda, *Org. Biomol. Chem.*, 2024, **22**, 6282–6287.
- 4 C. B. Nichinde, B. R. Patil, S. S. Chaudhari, B. P. Mali, R. G. Gonnade and A. K. Kinage, *RSC Adv.*, 2023, **13**, 13206–13212.
- 5 P. Paira, A. Hazra, S. Kumar, R. Paira, K. B. Sahu, S. Naskar, P. Saha, S. Mondal, A. Maity, S. Banerjee and N. B. Mondal, *Bioorg. Med. Chem. Lett.*, 2009, **19**, 4786–4789.
- 6 A. R. Karimi, Z. Dalirnasab, G. H. Yousefi and A. R. Akbarzadeh, *Res. Chem. Intermed.*, 2015, **41**, 10007–10016.
- 7 J. Gupta, A. Ahuja and R. Gupta, *Anti-Cancer Agents Med. Chem.*, 2022, **22**, 101–114.
- 8 G. Wang, J. Wang, Z. Xie, M. Chen, L. Li, Y. Peng, S. Chen, W. Li and B. Deng, *Bioorg. Chem.*, 2017, **72**, 228–233.
- 9 M. Santoso, L. L. Ong, N. P. Aijijiyah, F. A. Wati, A. Azminah, R. M. Annuur, A. Fadlan and Z. M. A. Judeh, *Heliyon*, 2022, **8**, e09045.



- 10 A. Natarajan, Y. H. Fan, H. Chen, Y. Guo, J. Iyasere, F. Harbinski, W. J. Christ, H. Aktas and J. A. Halperin, *J. Med. Chem.*, 2004, **47**, 1882–1885.
- 11 S. Kaur, J. Kaur, K. Kaur, R. Mahajan, Jyotisina and K. Kaur, *Curr. Indian Sci.*, 2024, **2**, e2210299X310595.
- 12 M. S. Christodoulou, F. Nicoletti, K. Mangano, M. A. Chiacchio, G. Facchetti, I. Rimoldi, E. M. Beccalli and S. Giofrè, *Bioorg. Med. Chem. Lett.*, 2020, **30**, 126845.
- 13 H. B. Rasmussen and J. K. MacLeod, *J. Nat. Prod.*, 1997, **60**, 1152–1154.
- 14 Y. A. Tayade, D. R. Patil, Y. B. Wagh, A. D. Jangle and D. S. Dalal, *Tetrahedron Lett.*, 2015, **56**, 666–673.
- 15 S. B. Gohain, M. Basumatary, P. K. Boruah, M. R. Das and A. J. Thakur, *Green Chem.*, 2022, **24**, 5338.
- 16 S. K. Guchhait, V. Chaudhary, V. A. Rana, G. Priyadarshani, S. Kandekar and M. Kashyap, *Org. Lett.*, 2016, **18**, 1534–1537.
- 17 H. Xu, S. Yamaguchi, T. Mitsudome and T. Mizugaki, *Eur. J. Org. Chem.*, 2022, **2022**, e202200826.
- 18 S. Banu, S. Choudhari, G. Patel and P. P. Yadav, *Green Chem.*, 2021, **23**, 3039–3047.
- 19 L. T. Cheng, S. Q. Luo, B. C. Hong, C. L. Chen, W. S. Li and G. H. Lee, *Org. Biomol. Chem.*, 2020, **18**, 6247–6252.
- 20 K. Rad-Moghadam, M. Sharifi-Kiasaraie and H. Taheri-Amlashi, *Tetrahedron*, 2010, **66**, 2316–2321.
- 21 K. X. Wu, Y. Z. Xu, L. Cheng, R. S. Wu, P. Z. Liu and D. Z. Xu, *Green Chem.*, 2021, **23**, 8448–8452.
- 22 P. Kamboj and V. Tyagi, *Green Chem.*, 2023, **26**, 1990–1999.
- 23 G. Brahmachari and B. Banerjee, *ACS Sustain. Chem. Eng.*, 2014, **2**, 2802–2812.
- 24 J. Azizian, A. A. Mohammadi, N. Karimi, M. R. Mohammadzadeh and A. R. Karimi, *Catal. Commun.*, 2006, **7**, 752–755.
- 25 Y. Sarrafi, K. Alimohammadi, M. Sadatshahabi and N. Norozipoor, *Monatsh. Chem.*, 2012, **143**, 1519–1522.
- 26 B. Suresh, G. Brahmeshwary, T. Swamy, I. Gopi and V. Ravinder, *Russ. J. Gen. Chem.*, 2016, **86**, 1144–1150.
- 27 H. Alinezhad, A. H. Haghghi and F. A. Salehian, *Chin. Chem. Lett.*, 2010, **21**, 183–186.
- 28 X. Yuan, S. Wang, J. Cheng, B. Yu and H. M. Liu, *Chin. Chem. Lett.*, 2020, **31**, 2465–2468.
- 29 A. Kamal, Y. V. V. Srikanth, M. N. A. Khan, T. B. Shaik and M. Ashraf, *Bioorg. Med. Chem. Lett.*, 2010, **20**, 5229–5231.
- 30 S. Y. Wang and S. J. Ji, *Tetrahedron*, 2006, **62**, 1527–1535.
- 31 K. Nikoofar, M. Haghghi and Z. Khademi, *Arab. J. Chem.*, 2019, **12**, 3776–3784.
- 32 R. K. Sharma and C. Sharma, *J. Mol. Catal. A: Chem.*, 2010, **332**, 53–58.
- 33 N. Edayadulla, N. Basavegowda and Y. R. Lee, *J. Ind. Eng. Chem.*, 2015, **21**, 1365–1372.
- 34 F. Lin, Y. Chen, B. Wang, W. Qin and L. Liu, *RSC Adv.*, 2015, **5**, 37018–37022.
- 35 G. K. Rastogi, B. Deka, M. L. Deb and P. K. Baruah, *Asian J. Org. Chem.*, 2022, **11**, 2–8.
- 36 B. V. S. Reddy, N. Rajeswari, M. Sarangapani, Y. Prashanthi, R. J. Ganji and A. Addlagatta, *Bioorg. Med. Chem. Lett.*, 2012, **22**, 2460–2463.
- 37 R.-P. Li, Z.-L. Wang, Y.-H. Zhang, Z.-Y. Tan and D.-Z. Xu, *ChemistrySelect*, 2022, **7**, 202200558.
- 38 H. Togo and S. Iida, *Synlett*, 2006, **14**, 2159–2175.
- 39 N. Anugu, S. Thunga, S. Golla and H. P. Kokatla, *Adv. Synth. Catal.*, 2022, **364**, 149–157.
- 40 CCDC 2490627: Experimental Crystal Structure Determination, 2026, DOI: [10.5517/ccdc.csd.cc2plptt](https://doi.org/10.5517/ccdc.csd.cc2plptt).

